Medical Image Analysis

Angshuman Paul

Assistant Professor

Department of Computer Science & Engineering

CT Image Analysis

Abdominal CT: Lesion Detection, Tagging & Segmentation

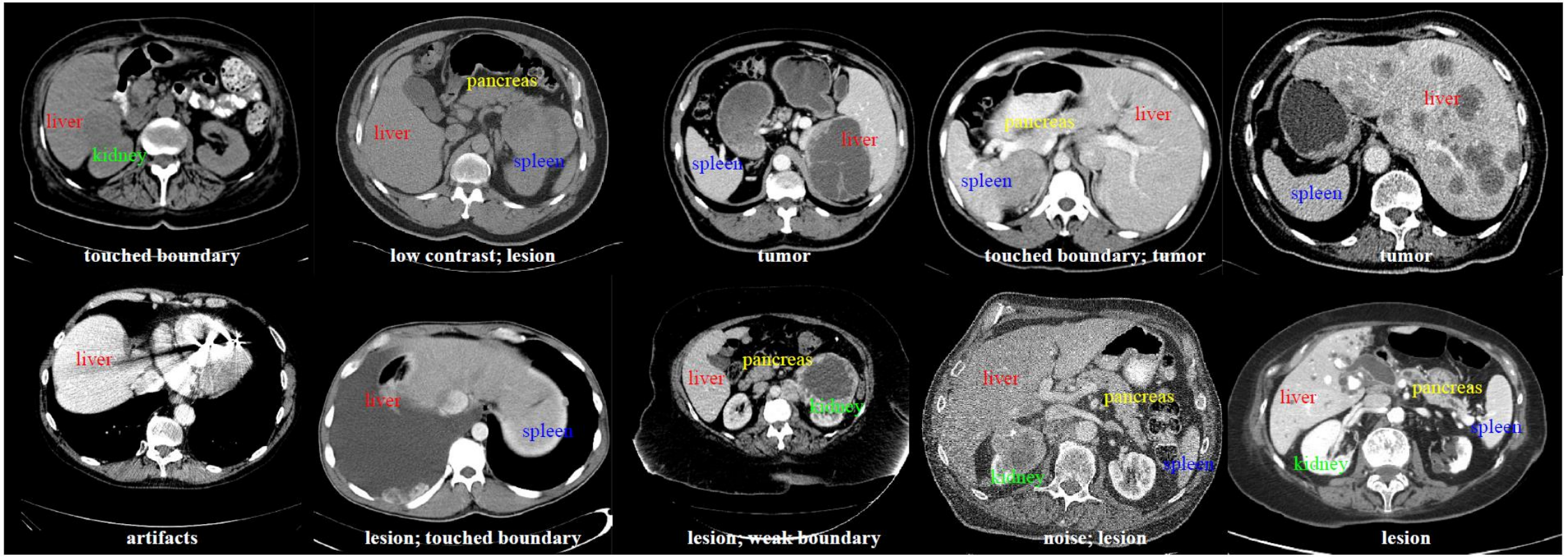

https://arxiv.org/abs/2010.14808

3D Information Fusion

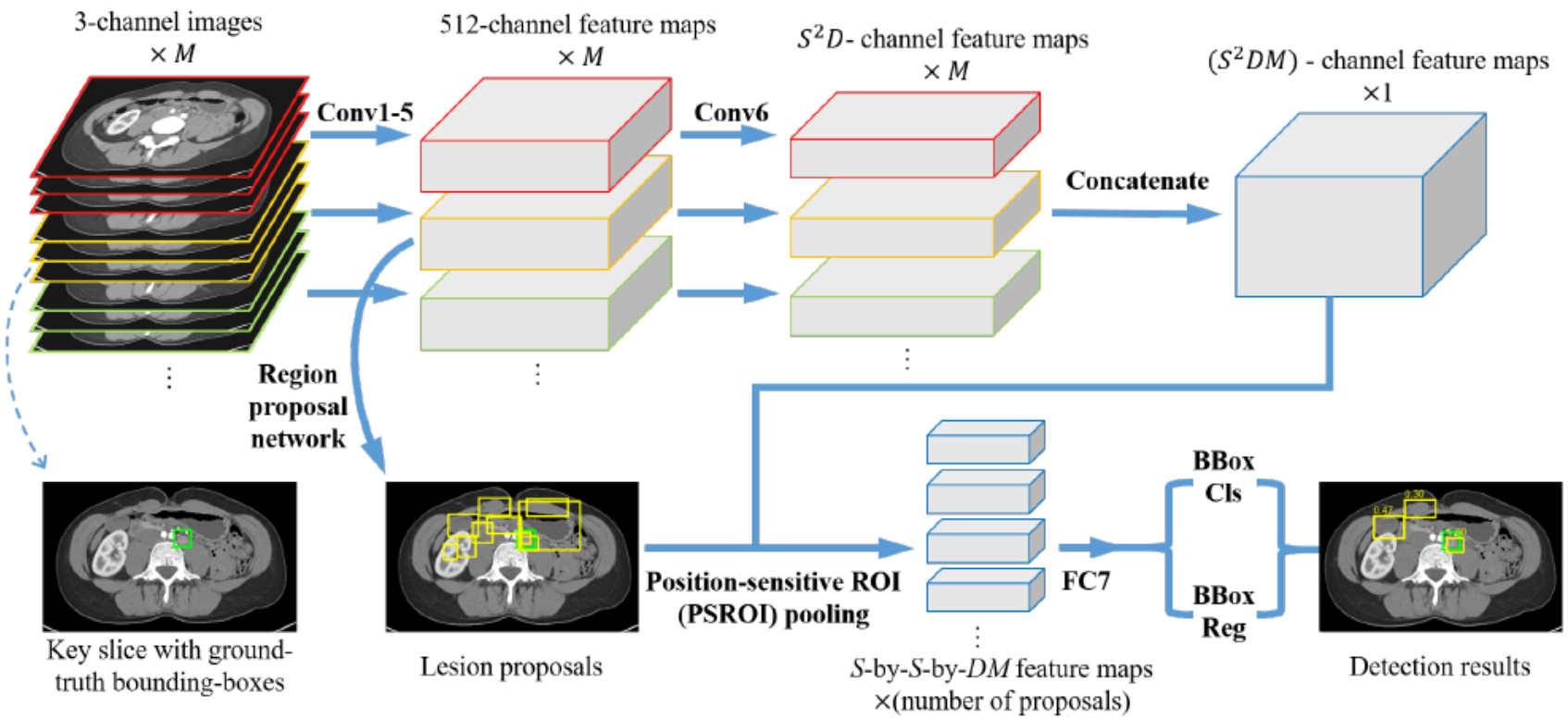

3DCE

https://arxiv.org/abs/1806.09648

3D Information Fusion

- Modified Mask R CNN

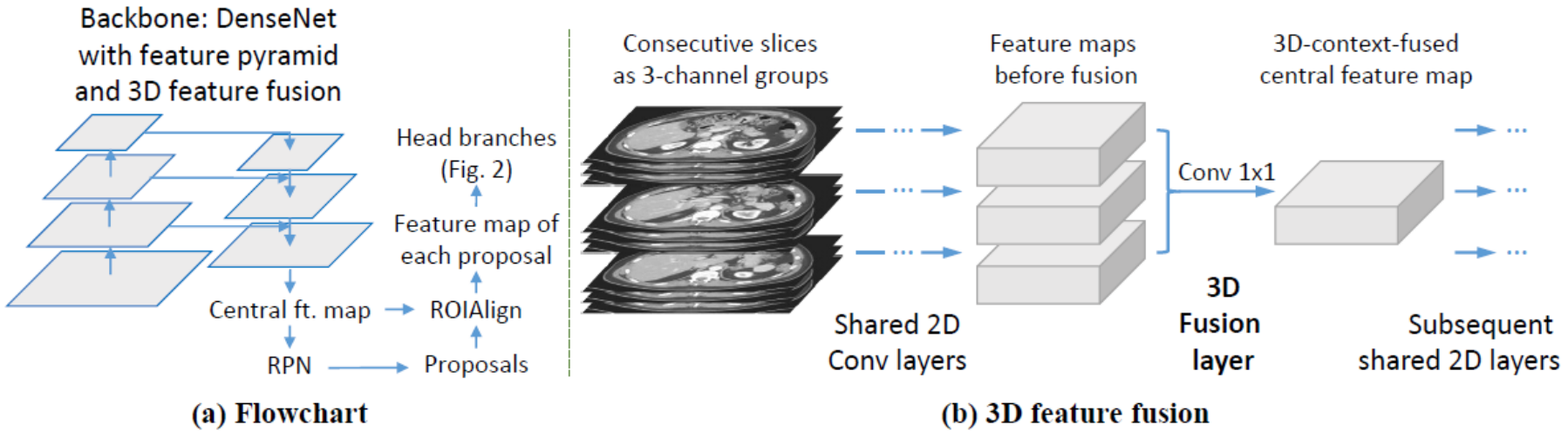

MULAN

https://arxiv.org/abs/1908.04373

3D Information Fusion

- Modified Mask R CNN

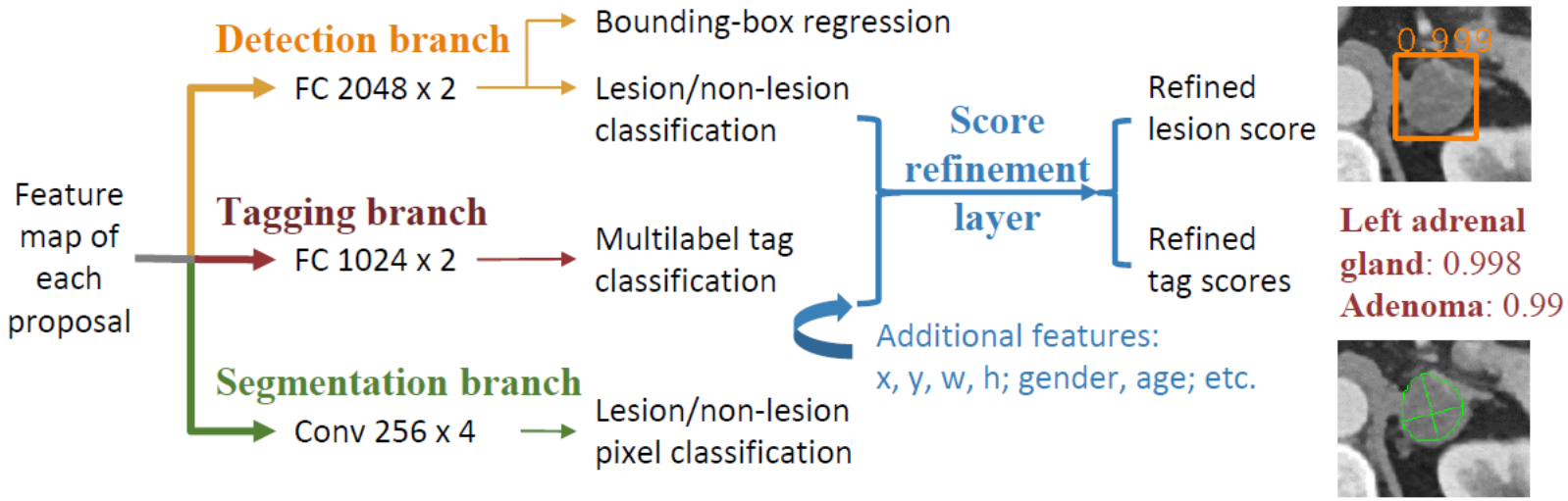

MULAN

https://arxiv.org/abs/1908.04373

MULAN

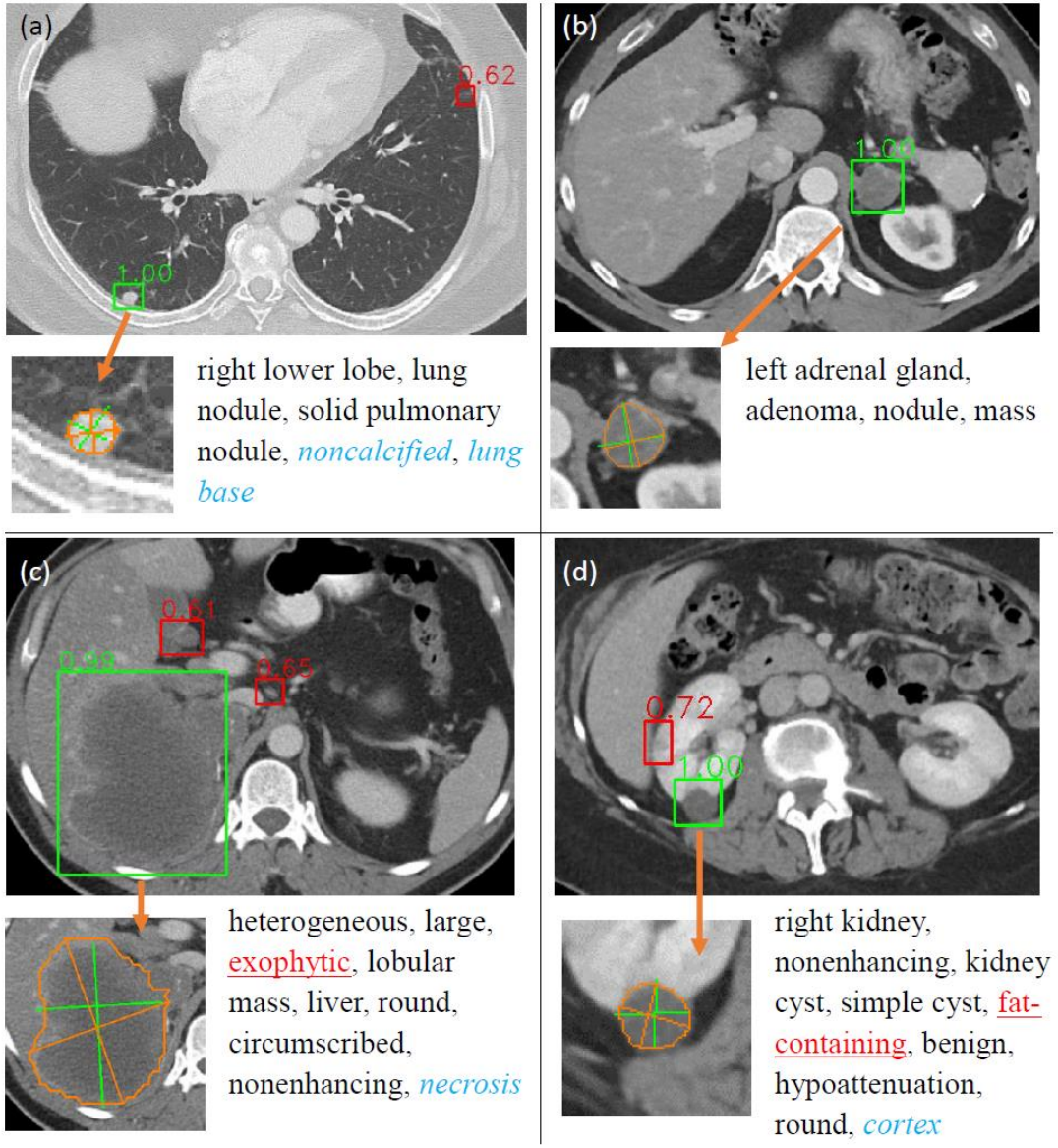
(a)
0.62
1.00
right lower lobe, lung nodule, solid pulmonary nodule, noncalcified, lung base
(b)
1.00
left adrenal gland, adenoma, nodule, mass
(c)
0.61
0.99
0.65
heterogeneous, large, exophytic, lobular mass, liver, round, circumscribed, nonenhancing, necrosis
(d)
0.72
1.00
right kidney, nonenhancing, kidney cyst, simple cyst, fat-containing, benign, hypoattenuation, round, cortex

Pancreas Segmentation from NC CT Images

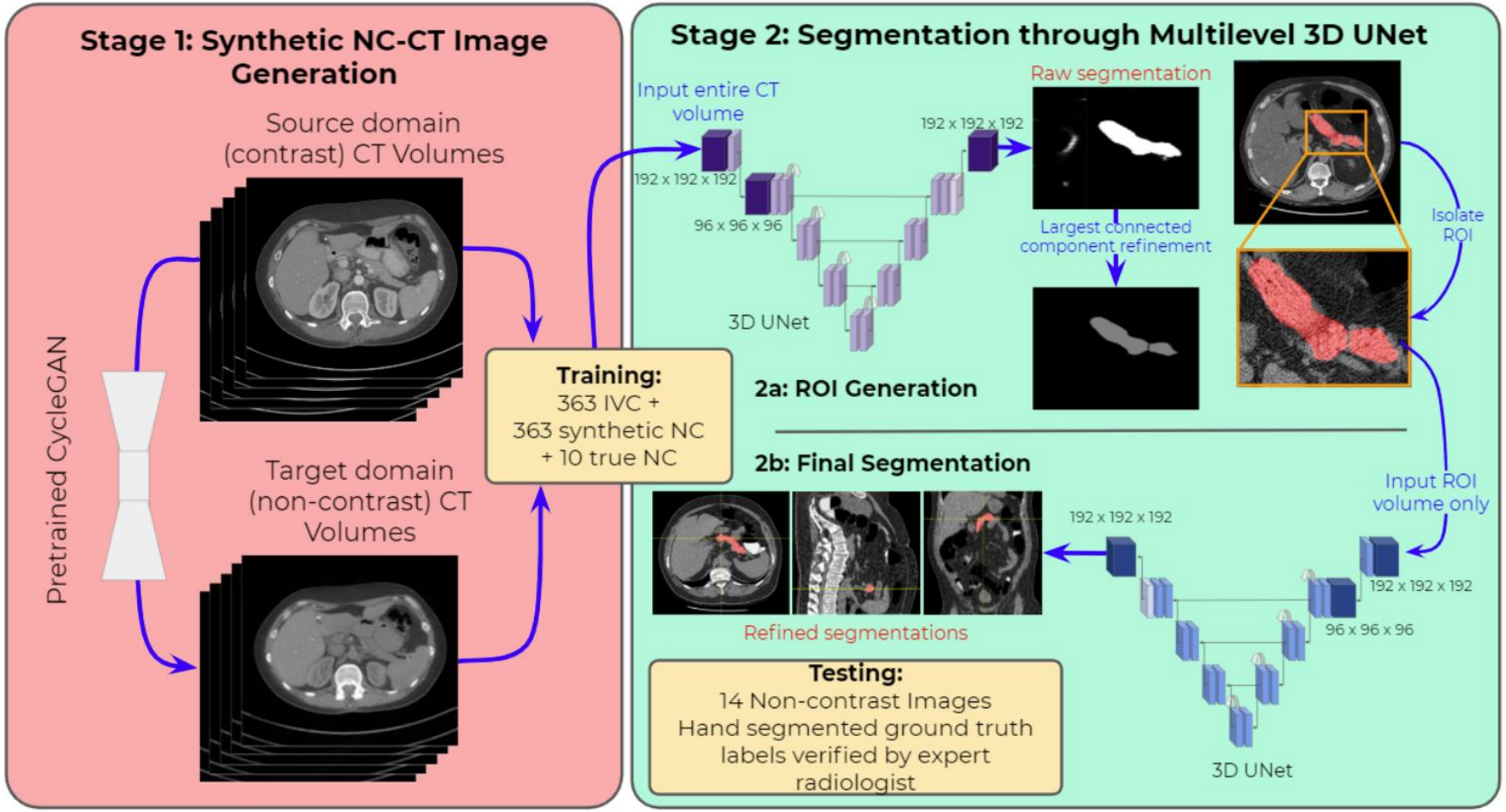

Datasets

- LiTS (Liver, segmentation mask)
- KiTs (Kidney and kidney tumor)
- DeepLesion (Multi-organ, no segmentation mask, RECIST measurement, tags)
- AbdomenCT-1K (https://arxiv.org/abs/2010.14808)

RECIST: Response evaluation criteria in solid tumors

Liver Datasets

Table 1
Overview of publicly available medical datasets of liver and liver tumor images. The LiTS dataset offers a comparably large amount of 3D scans, including liver and liver tumor annotations.

Dataset	Institution	Liver	Tumor	Segmentation	#Volumes	Modality
TCGA-LIHC (Erickson et al., 2016)	TCIA	✓	✓	✗	1688	CT, MR, PT
MIDAS (Cleary, 2017)	IMAR	✓	✓	✗	4	CT
3Dircadb-01 and 3Dircadb-02 (Soler et al., 2010)	IRCAD	✓	✓	✓	22	CT
SLIVER'07 (Heimann et al., 2009)	DKFZ	✓	✗	✓	30	CT
LTSC'08 (Heimann et al., 2009)	Siemens	✗	✓	✓	30	CT
ImageCLEF'15 ()	Bogazici Uni.	✓	✗	✓	30	CT
VISCERAL'16 (Jimenez-del Toro et al., 2016)	Uni. of Geneva	✓	✗	✓	60/60	CT/MRI
CHAOS'19 (Kavur et al., 2021)	Dokuz Eylul Uni.	✓	✗	✓	40/120	CT/MRI
LiTS	TUM	✓	✓	✓	**201**	CT

LiTS Dataset: Sample Results

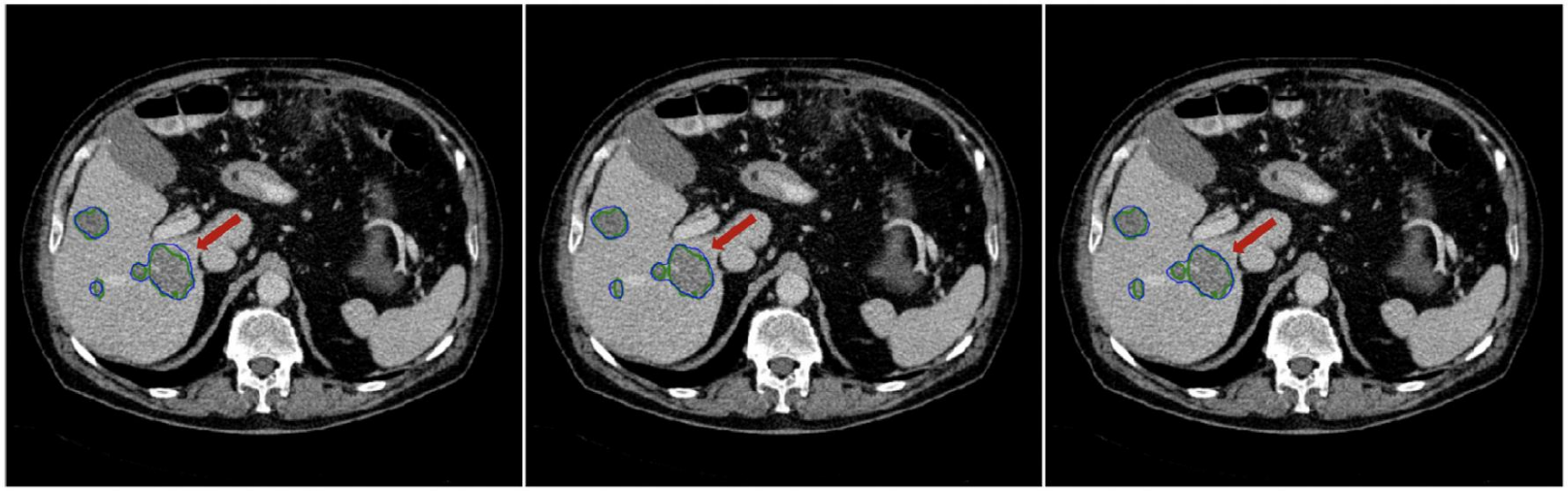

Han *et al.* Vorontsov *et al.* Bi *et al.*

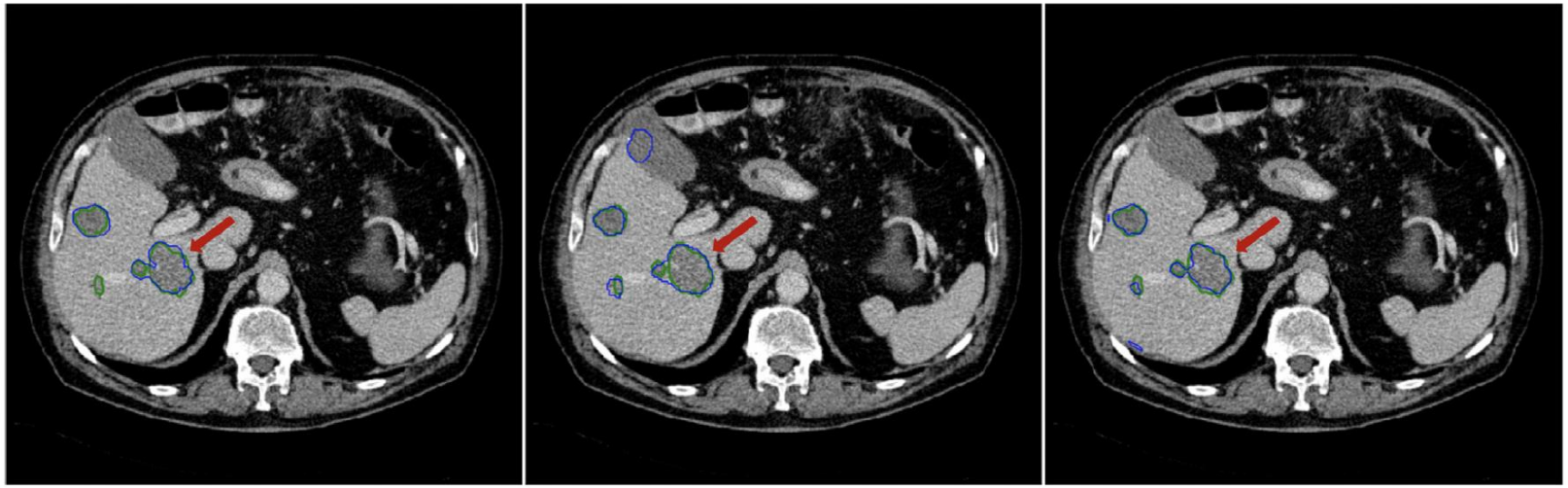

Ma *et al.* Wang *et al.* Lipkova *et al.*

AbdomenCT-1K: Sample Results

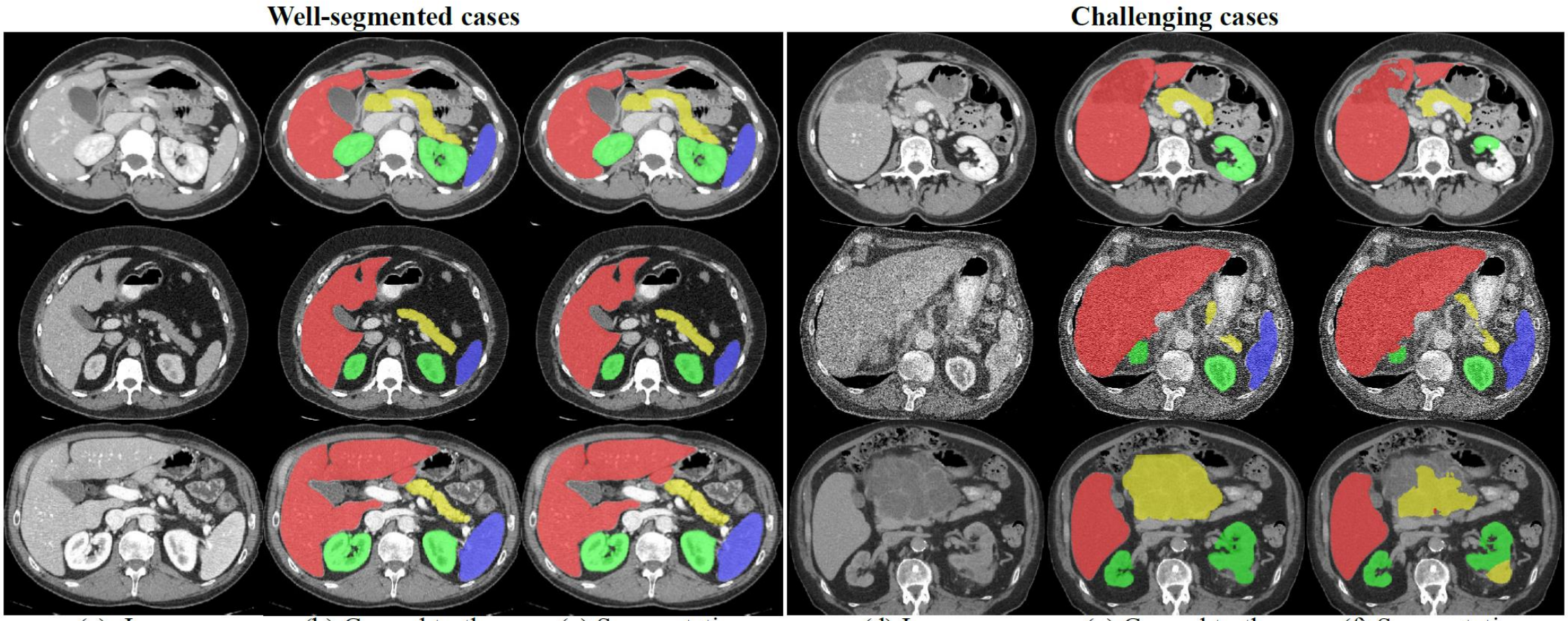

nnU-Net

nnU-Net

- No new net
  - Not a new network architecture, loss function or training scheme
- Systematizing the complex process of manual method configuration
- Distillation of knowledge from a large pool of datasets into a set of robust design choices that translates into powerful inductive biases when applied to a new dataset

https://www.nature.com/articles/s41592-020-01008-z

nnU-Net

- Collect design decisions that do not require adaptation between datasets and identify a robust common configuration (‘fixed parameters’).

- For as many of the remaining decisions as possible, formulate explicit dependencies between specific dataset properties (‘dataset fingerprint’) and design choices (‘pipeline fingerprint’) in the form of heuristic rules to allow for almost-instant adaptation on application (‘rule-based parameters’).

- Learn only the remaining decisions empirically from the data (‘empirical parameters’).

https://www.nature.com/articles/s41592-020-01008-z

nnU-Net

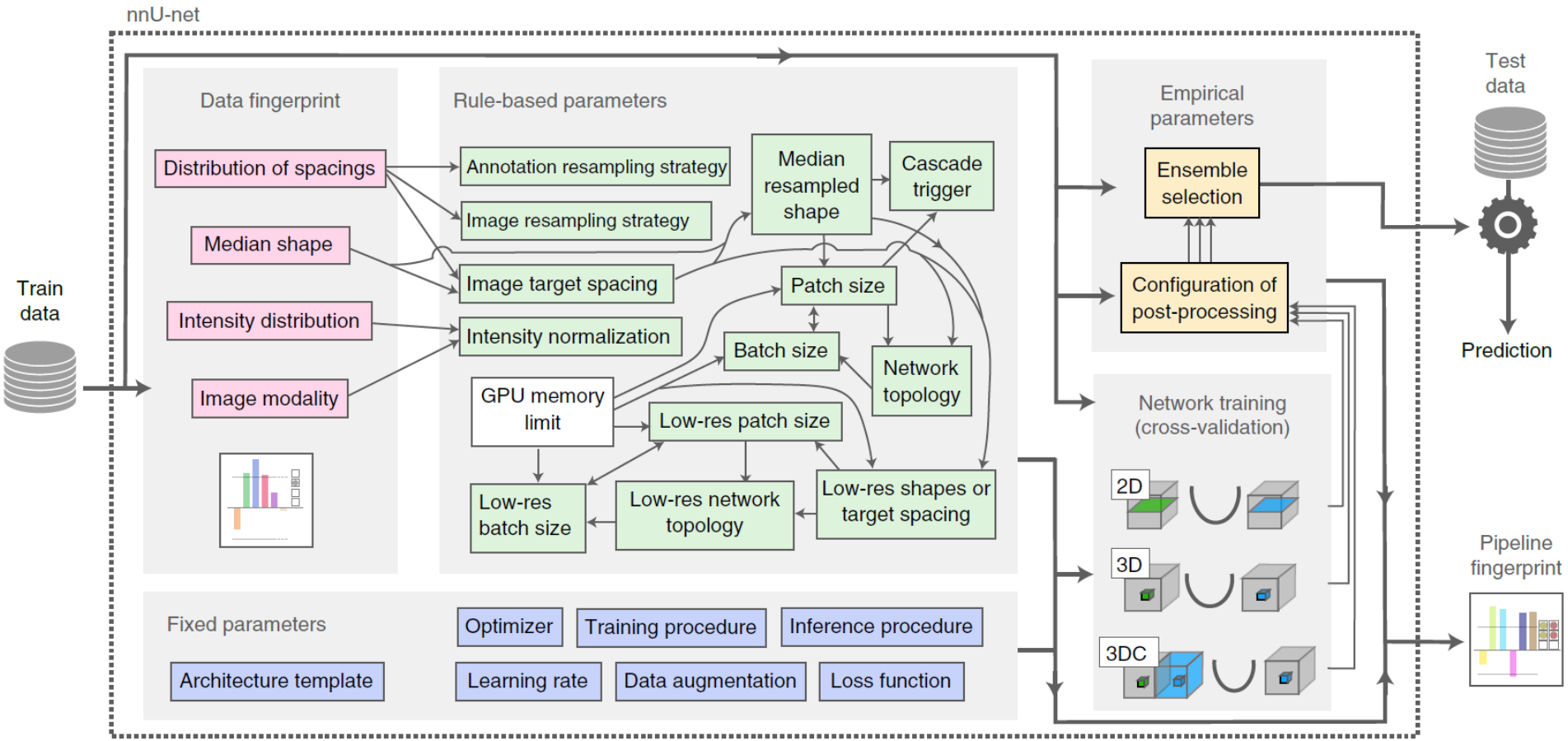

https://www.nature.com/articles/s41592-020-01008-z

nnU-Net

Design choice	Required input	Automated (fixed, rule-based or empirical) configuration derived by distilling expert knowledge (more details in online methods)
Learning rate	–	Poly learning rate schedule (initial, 0.01)
Loss function	–	Dice and cross-entropy
Architecture template	–	Encoder–decoder with skip-connection ('U-Net-like') and instance normalization, leaky ReLU, deep supervision (topology-adapted in inferred parameters)
Optimizer	–	SGD with Nesterov momentum ($\mu = 0.99$)
Data augmentation	–	Rotations, scaling, Gaussian noise, Gaussian blur, brightness, contrast, simulation of low resolution, gamma correction and mirroring
Training procedure	–	1,000 epochs × 250 minibatches, foreground oversampling
Inference procedure	–	Sliding window with half-patch size overlap, Gaussian patch center weighting
Intensity normalization	Modality, intensity distribution	If CT, global dataset percentile clipping & z score with global foreground mean and s.d. Otherwise, z score with per image mean and s.d.
Image resampling strategy	Distribution of spacings	If anisotropic, in-plane with third-order spline, out-of-plane with nearest neighbor Otherwise, third-order spline
Annotation resampling strategy	Distribution of spacings	Convert to one-hot encoding → If anisotropic, in-plane with linear interpolation, out-of-plane with nearest neighbor Otherwise, linear interpolation
Image target spacing	Distribution of spacings	If anisotropic, lowest resolution axis tenth percentile, other axes median. Otherwise, median spacing for each axis. (computed based on spacings found in training cases)
Network topology, patch size, batch size	Median resampled shape, target spacing, GPU memory limit	Initialize the patch size to median image shape and iteratively reduce it while adapting the network topology accordingly until the network can be trained with a batch size of at least 2 given GPU memory constraints. for details see online methods.
Trigger of 3D U-Net cascade	Median resampled image size, patch size	Yes, if patch size of the 3D full resolution U-Net covers less than 12.5% of the median resampled image shape
Configuration of low-resolution 3D U-Net	Low-res target spacing or image shapes, GPU memory limit	Iteratively increase target spacing while reconfiguring patch size, network topology and batch size (as described above) until the configured patch size covers 25% of the median image shape. For details, see online methods.
Configuration of post-processing	Full set of training data and annotations	Treating all foreground classes as one; does all-but-largest-component-suppression increase cross-validation performance? Yes, apply; reiterate for individual classes No, do not apply; reiterate for individual foreground classes
Ensemble selection	Full set of training data and annotations	From 2D U-Net, 3D U-Net or 3D cascade, choose the best model (or combination of two) according to cross-validation performance

https://www.nature.com/articles/s41592-020-01008-z

nnU-Net

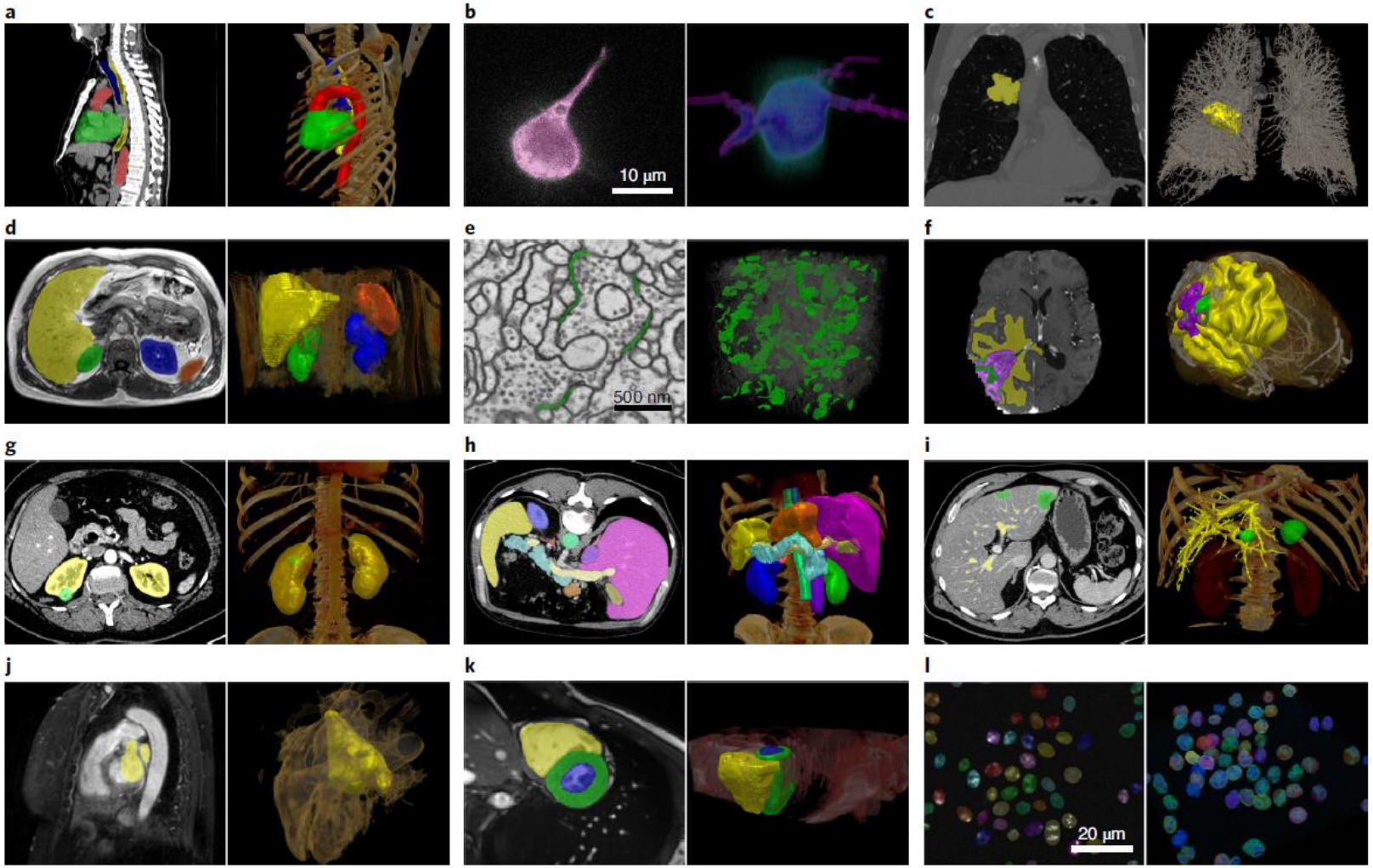

Fig. 1 | nnU-Net handles a broad variety of datasets and target image properties. All examples originate from test sets of different international segmentation challenges to which nnU-Net was applied. Target structures for each dataset are shown in 2D projected onto the raw data (left) and in 3D together with a volume rendering of the raw data (right). All visualizations were created with the MITK Workbench[35]. **a**, Heart (green), aorta (red), trachea (blue) and esophagus (yellow) in CT images (dataset (D)18)[14]. **b**, A549 lung cancer cells (purple) in FM (D22)[36,37]. **c**, Lung nodules (yellow) in CT images (D6)[14]. **d**, Liver (yellow), spleen (orange), left and right kidneys (blue and green, respectively) in T1 in-phase MRI (D16)[20]. **e**, Synaptic clefts (green) in EM scans (D19) (https://cremi.org/). **f**, Edema (yellow), enhancing tumor (purple), necrosis (green) in MRI (T1, T1 with contrast agent, T2, FLAIR) (D1)[14,38]. **g**, Kidneys (yellow) and kidney tumors (green) in CT images (D17)[21]. **h**, Thirteen abdominal organs in CT images (D11)[16]. **i**, Hepatic vessels (yellow) and liver tumors (green) in CT (D8)[14]. **j**, Left ventricle (yellow) in MRI (D2)[14]. **k**, Right ventricle (yellow), left ventricular cavity (blue) and myocardium of left ventricle (green) in cine MRI (D13)[6]. **l**, HL60 cell nuclei (instance segmentation, one color per instance) in FM (D21)[39].

COVID-19 Diagnosis

COVID-19

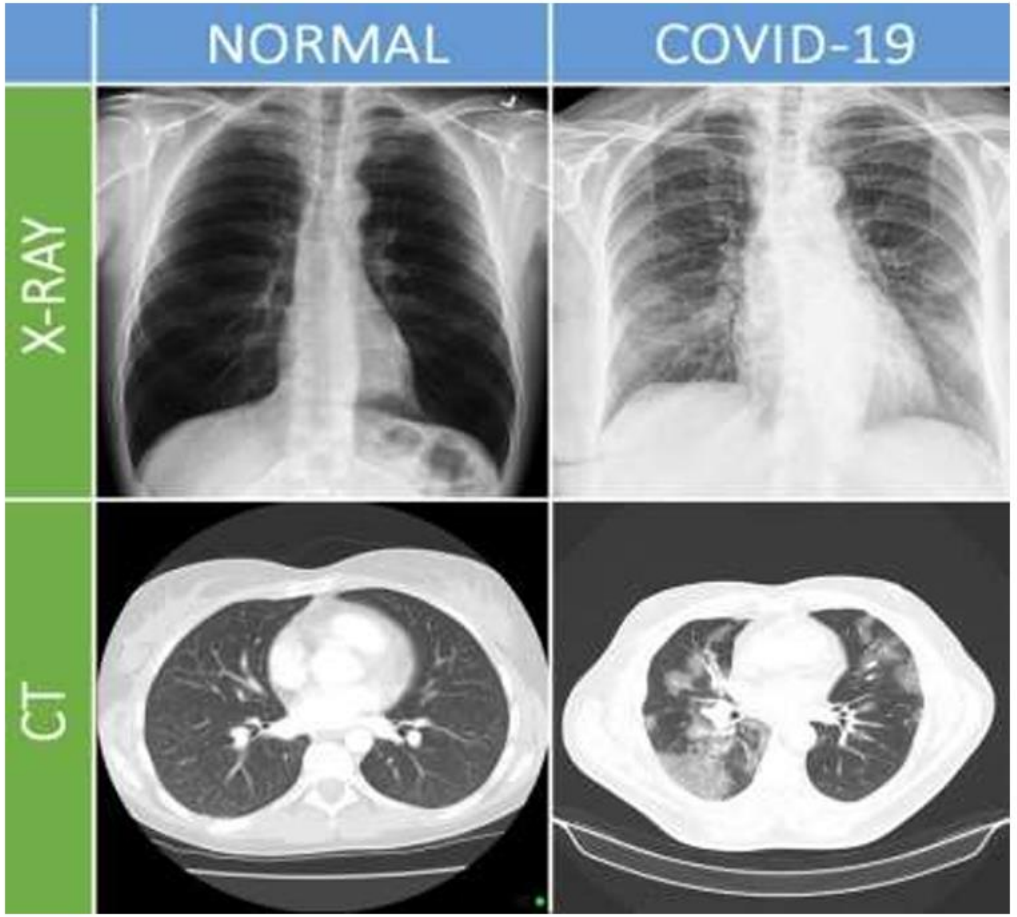

https://arxiv.org/ftp/arxiv/papers/2202/2202.06372.pdf

COVID-19

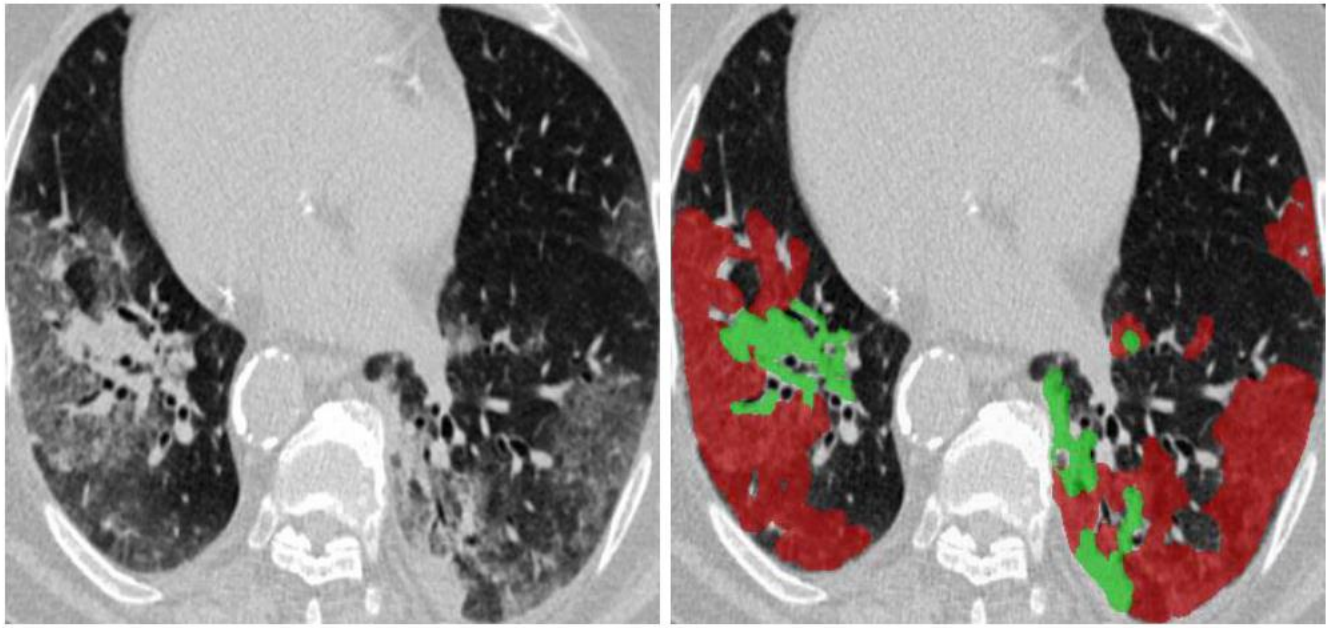

(A) (B)

Fig. 1. Example of COVID-19 infected regions (B) in CT axial slice (A), where the red and green masks denote the GGO and consolidation, respectively. The images are collected from [9].

GGO: Ground Glass Opacity

https://ieeexplore.ieee.org/stamp/stamp.jsp?tp=&arnumber=9098956

COVID-19

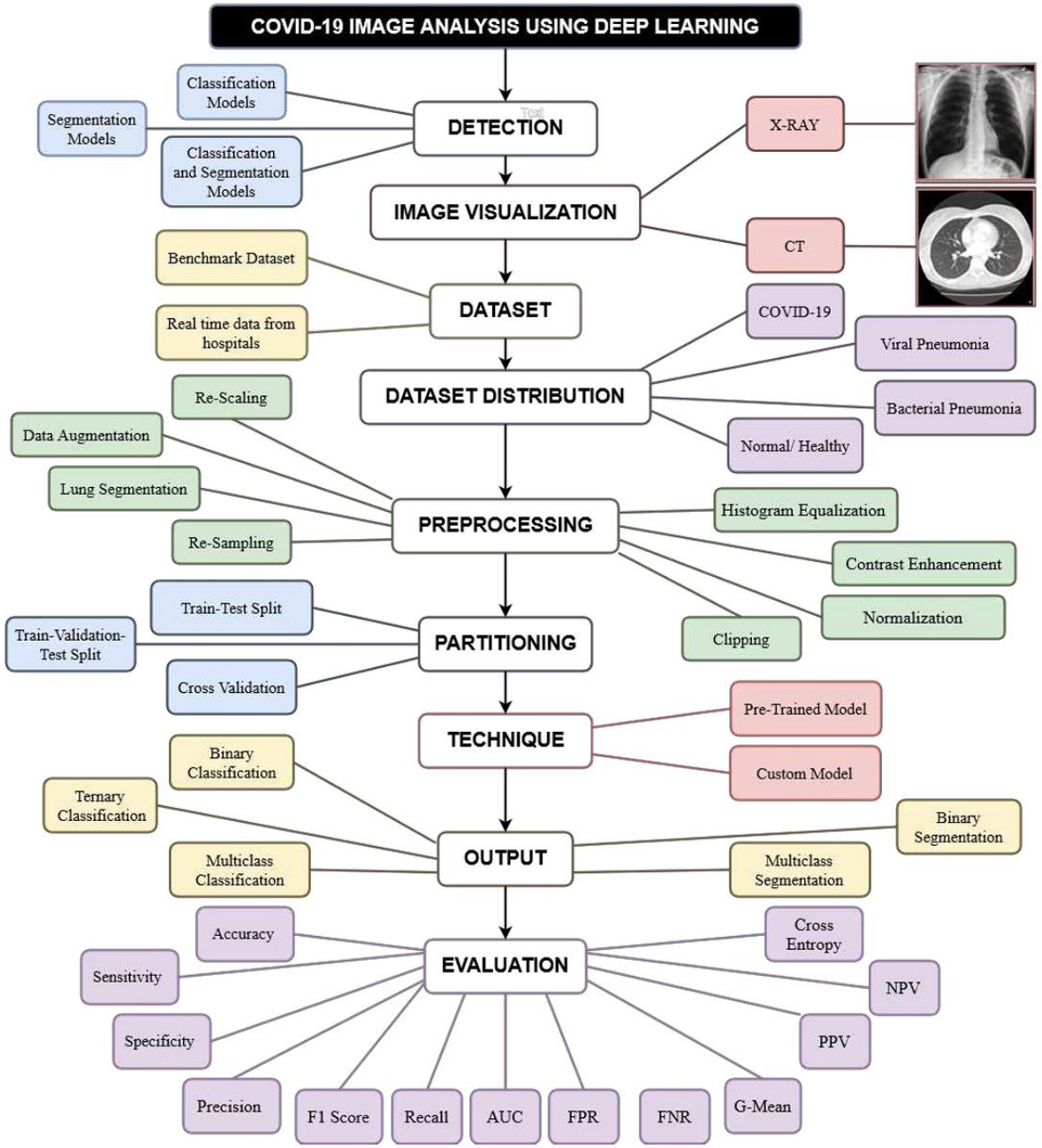

https://arxiv.org/ftp/arxiv/papers/2202/2202.06372.pdf

COVID-19: Custom Models for CT

Ref.	Data Sources and Cross-Validation	Technique	Classes	Performance
Wang et al.[51] 46	Dataset acquired using Philips Ingenuity 64 row spiral CT machine (90:10%) Hold-out CV	**FGCNet,** RBFNN [104] RCBBO [108] ,COVNet [109]	Binary	ACC = 97.14%, F1-score = 97.2%, MCC = 94.3%, SEN = 97.7%, PRE= 96.6%, SPEC = 96.6%, FMI = 97.2%.
Singh et al. [95]	Dataset [105] Kaggle CXR data [77]	**MODE-based CNN Model** ANN, ANFIS	Binary	ACC = 97.9%, F1-Score = 98.0% (20:80%) 10-Fold CV

https://arxiv.org/ftp/arxiv/papers/2202/2202.06372.pdf

COVID-19: Custom Models for CT

Ref.	Data Sources and Cross-Validation	Technique	Classes	Performance
Wang et al.[51] 46	Dataset acquired using Philips Ingenuity 64 row spiral CT machine (90:10%) Hold-out CV	**FGCNet,** RBFNN [104] RCBBO [108] ,COVNet [109]	Binary	ACC = 97.14%, F1-score = 97.2%, MCC = 94.3%, SEN = 97.7%, PRE= 96.6%, SPEC = 96.6%, FMI = 97.2%.
Singh et al. [95]	Dataset [105] Kaggle CXR data [77]	**MODE-based CNN Model** ANN, ANFIS	Binary	ACC = 97.9%, F1-Score = 98.0% (20:80%) 10-Fold CV

https://arxiv.org/ftp/arxiv/papers/2202/2202.06372.pdf

COVID-19: Custom Models for CT

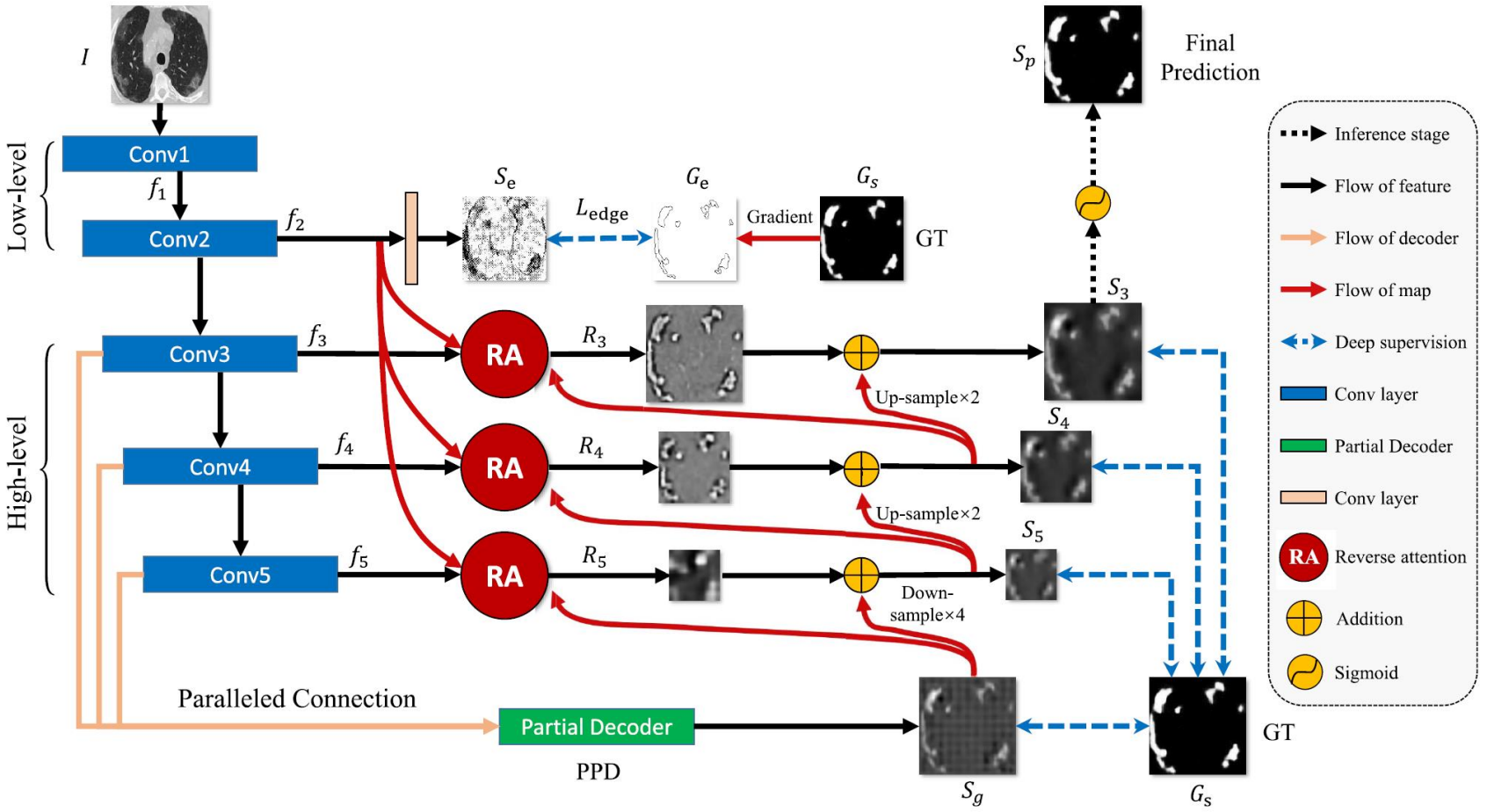

Fig. 2. The architecture of our proposed *Inf-Net* model, which consists of three reverse attention (RA) modules connected to the paralleled partial decoder (PPD). See § III-A for details.

https://ieeexplore.ieee.org/stamp/stamp.jsp?tp=&arnumber=9098956

COVID-19: Custom Models for CT

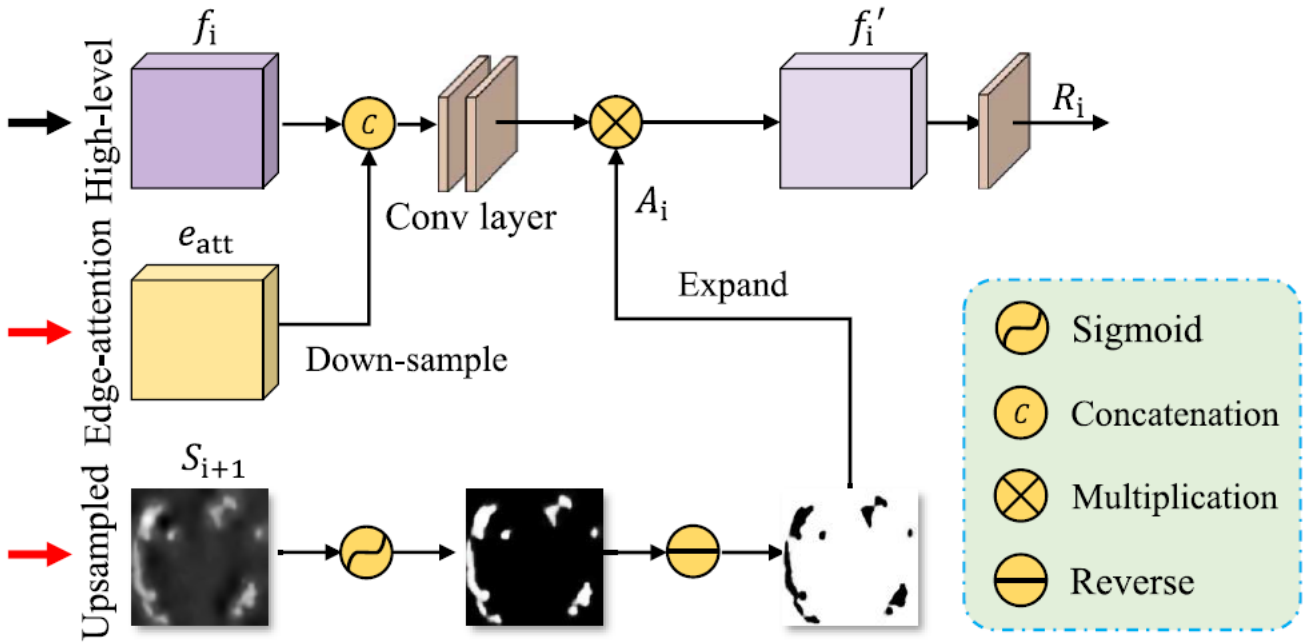

Fig. 4. Reverse attention module is utilized to implicitly learning edge features.

https://ieeexplore.ieee.org/stamp/stamp.jsp?tp=&arnumber=9098956